Backlash Identification in Industrial Positioning Systems Aided by a Mobile Accelerometer Board with Wi-Fi

Mathias Tantau[1][a], Lars Perner[2], Mark Wielitzka[1][b] and Tobias Ortmaier[1][c]

[1]*Institute of Mechatronic Systems, Leibniz University Hanover, An der Universität 2, 30823 Garbsen, Germany*
[2]*Lenze Automation GmbH, Am Alten Bahnhof 11, D-38122 Braunschweig, Germany*

Keywords: Backlash Identification, Accelerometer, Electric Drives, Electric Power Trains.

Abstract: In electromechanical motion systems performance measures such as positioning accuracy, dynamic stiffness and control bandwidth are severely limited by backlash. Several control schemes based on backlash compensation or switching control of hybrid systems are known, but many of these approaches require the exact backlash width as an input parameter. Several existing approaches for backlash identification are limited in accuracy because the load-side velocity is required but it is not directly measurable. In this paper a method for backlash identification tailored to electromechanical motion systems with rotary motor and translationally moving load is proposed. A mobile sensor board with inertial measurement unit (IMU) is mounted temporarily on the load and serves to acquire the accelerations during the experiment. The connection to the host-PC is wireless, time synchronisation is not required. It is shown in experiments on a testbed with an adjustable backlash coupling but otherwise industry-like equipment that high accuracies can be achieved.

1 INTRODUCTION

Electric drives in automation industry are required to have a high closed-loop bandwidth and a high dynamic stiffness in response to external disturbances. Both is highly limited by backlash between the motor inertia and the load inertia. Backlash, also called deadzone, is present in many drive systems, mainly emerging from gear play.

A number of control metrics have been developed for systems with backlash (Lagerberg, 2001; Nordin and Gutman, 2002). Many of them consider the backlash gap width explicitly in the design although this parameter is often unknown and changes over time. Examples are given in the following paragraph.

An early work on control of systems with backlash is the one by Tao and Kokotovic (Tao and Kokotovic, 1996). Three different methods of exact linearisation control depending on the availability of angle sensors at the drive side and/or load side are demonstrated in (Schoeling and Orlik, 2000). The backlash width is required in the design. Friedland (Friedland, 1997) developed a load side observer that requires

[a] https://orcid.org/0000-0003-1195-7329
[b] https://orcid.org/0000-0003-0088-6457
[c] https://orcid.org/0000-0003-1644-3685

knowledge of the backlash gap size and the load inertia. A concept based on model predictive control was developed by Lagerberg and Egardt (Lagerberg and Egardt, 2005) that requires knowledge of the exact backlash width. The controller by Nordin and Gutman (Nordin and Gutman, 2000) softly switches between a mode for operation in the backlash gap and a mode with high gain for operation in contact with the load. The switching rule requires knowledge of the backlash width and the stiffness. In (Rostalski et al., 2007) model predictive control with state observer is proposed for systems with backlash. It is shown in experiments that uncertainty in the required model parameters such as the backlash width limits the performance considerably or respectively leads to instability. A backlash compensation control scheme for twin-drive systems with backlash is proposed in (Itoh, 2008), that requires the backlash width as an input parameter.

In summary, the explicit consideration of nonlinearities like backlash and friction improves performance (Marton and Lantos, 2009), but often these advanced approaches cannot be put into practice because the required backlash width is not known.

This explains the quest for backlash identification methods that cannot only detect its presence in the sense of condition monitoring and fault diagnosis, but

can determine the exact value.

Existing works can mainly be divided into minimization of simulation model errors, extraction of features in the measured signals and online state and parameter observers. The first group can further be divided into time domain approaches and frequency domain approaches. Examples of the former are the works of (Ravanbod-Shirazi and Besançon-Voda, 2002; Zemke, 2012; Calvini et al., 2015), where backlash and other parameters are identified by time domain output error minimization with for example particle swarm as an optimizer. A frequency domain approach is the one presented by (Popp et al., 2019). Online observers are addressed in the works of Reddy (Reddy et al., 2019).

Feature-based methods detect the time instances when the backlash gap is entered and when it is left. These are also called commutation times (Ravanbod-Shirazi and Besançon-Voda, 2002) and mainly show up in the velocity and current signals of the motor, e.g. (Gebler and Holtz, 1998). The backlash parameter is obtained by integrating the velocity difference between motor and load. Details of the load-side velocity estimation and the detection of commutation times depend on the availability of sensors and other system parameters.

In (Marton and Lantos, 2009) it is utilized that the load stays at rest after a velocity reversal until the backlash gap is passed, so in this case the load-side velocity is known (zero). The re-engagement time is detected in the motor current. Villwock and Pacas (Villwock and Pacas, 2009) drive a triangular velocity and detect the commutation instances right after the maximum velocity peak by analysing the velocity signal. The load speed is assumed to be constant. Their technique can be refined by utilizing also the motor current signal, especially if the load friction is known (Han et al., 2016). The load deceleration can also be determined from the commutation times if a sinusoidal excitation is used instead of a triangular one (Specht, 1986) or if a load-side velocity sensor exists (Ravanbod-Shirazi and Besançon-Voda, 2002). Two methods based on the assumption of zero load velocity in backlash mode are compared in (Zhang et al., 2018). One of them detects the contact-separation-contact times via transmission torque mutations, the other method measures the load-side speed and uses a describing function to calculate the backlash angle from the phase lag of the load's base frequency.

The limitation of most of these methods is that certain assumptions about the load are made (constant load-speed, known friction) which are not satisfied in all applications and the true behaviour of the load is not known if no load-side sensor exists. In real-life applications it is expectable that the friction is not negligible and it is not measurable independent of the motor friction. Gravity is another problem. Load-side sensors could be installed but only at high costs and cabling efforts.

This paper aims at backlash identification for rotary motors by the help of a mobile, radio controlled sensor board based on an inertial measurement unit (IMU). It is attached temporarily to the linearly moving load and helps to reconstruct the load-side velocity. The main goal of the presented technique of this paper is to improve the identification accuracy based on these extra data. Installation effort is minimized because the sensor board transmits the measurements via Wi-Fi and it is battery-powered.

2 BACKLASH IDENTIFICATION

This section describes the proposed procedure of backlash identification for an electrical power train with belt drive as shown in Fig. 1. A controlled servo motor with angle or angular velocity sensor is connected to a translationally guided load by means of a belt drive, toothed rack and pinion, or a ball screw. In the figure a revolving belt drive is shown. Often, there is also a gearbox with backlash behind the motor. The gear ratio is i, the backlash angle is 2α and the feed constant of the translational element is c_f, e.g. $c_f = 2\pi R$ for the belt drive with pulley radius R. Such a configuration is encountered frequently in automation industry, for example in linear positioning systems, stacker cranes, rapid prototyping and machine tools. In contrast to testbeds with free-wheeling load the belt drive has considerable friction, but as an advantage the linear acceleration of the load $a(t)$ can be used as an additional input signal for backlash identification.
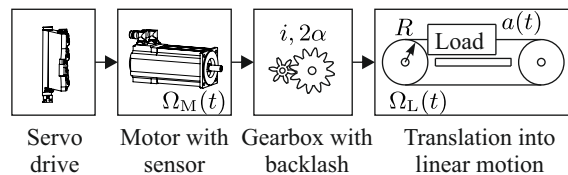

Figure 1: Drive train of electromechanical positioning system with rotary motor and linearly moving load.

The proposed procedure is developed along Fig. 2. Although the exact experimental setup is postponed till Sec. 3 this measurement for $10°$ serves already now as a demonstration. It is assumed for now that gravity has no influence, i.e. the linear motion is horizontal. Similar to the approach of Villwock (Villwock and Pacas, 2009) the motor is commanded to acceler-

ate up to a certain maximum velocity, followed by a sharp deceleration, as indicated in grey, $\Omega_{ref}(t)$. In red the actual motor speed is shown. In addition, the velocity of the load-side of the backlash element is given (green line). This signal is measured for visualization only and it is not used for backlash identification.
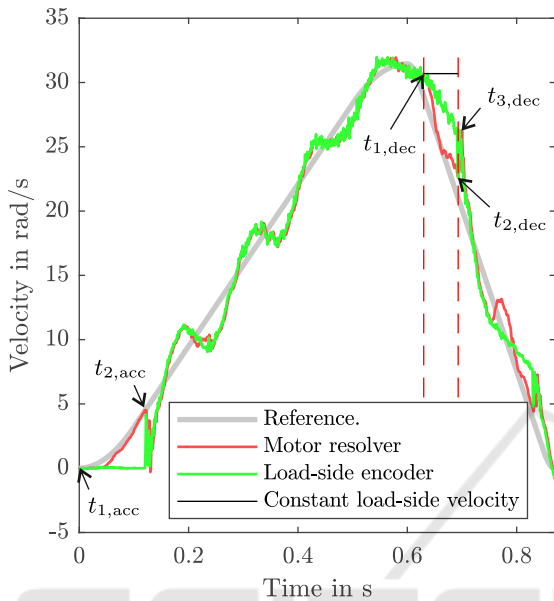

Figure 2: Velocities of an exemplary experiment with 10° backlash setting without acceleration sensor.

Due to our long-term goal of using the identified backlash for control design, all measurements are done with misadjusted control parameters. This leads to clearly observable oscillations after each backlash impact. The identification algorithm is robust enough to handle this suboptimal system behaviour.

There are two distinct patterns where the backlash becomes evident. In the beginning of the acceleration phase the load remains at rest while the motor accelerates already and traverses the backlash gap. This effect is utilized in (Marton and Lantos, 2009). When the impact with the load-side occurs, the motor velocity drops instantaneously to a value close to zero while simultaneously the load is accelerated. The second characteristic pattern is observed after the velocity peak has been passed in the deceleration phase. It can be seen that the motor decelerates faster than the load and a clear divergence between the two velocities occurs. At the other end of the backlash gap the motor re-engages with the load and is accelerated by the impact force. This effect is utilized in (Villwock and Pacas, 2009).

For backlash identification both patterns (acceleration and deceleration) can be evaluated as long as the commutation times can safely be recognized and the

load-side velocity can be approximated (Villwock and Pacas, 2009):

$$2\alpha = \left| \int_{t_1}^{t_2} \Omega_M(t) - \Omega_L(t) \mathrm{d}t \right|. \qquad (1)$$

Ω_M and Ω_L are the angular velocity of motor and load, respectively. t_1 and t_2 are the commutation times before and after backlash gap passing. They are replaced by the times with index acc and dec for acceleration and deceleration phase, respectively, see Fig. 2.

For fully automatic backlash identification, conditions for detecting the commutation times must be established. In the acceleration phase $t_{1,acc}$ coincides with $t = 0$. It is ensured by a slow backward movement preceding the experiment that the backlash element is actually at the one end, in a defined state when the shown velocity profile begins. $t_{2,acc}$ can be detected by a sharp drop in the motor velocity. Here, $t_{2,acc}$ is defined as the time instant in the acceleration phase when the maximum motor velocity is reached which is followed by a drop in the velocity of at least 50 % of this maximum.

50 % is the value expectable for bounce-free but undamped re-engagement by conservation of momentum if the inertia ratio of motor and load is 1. Usually, the load inertia exceeds the motor inertia, leading to a deeper drop and 50 % is a safe setting. On the other hand, if the load is lighter, backlash identification becomes less important for control design, because the control parameters are predominantly determined by the motor inertia.

In the deceleration phase $t_{1,dec}$ is defined as the time instant corresponding to the maximal motor velocity after the maximum in the reference speed has been reached (first dashed line in Fig. 2). $t_{2,dec}$ is more difficult to determine automatically. First, the maximum in $\Omega_M(t) - \Omega_{ref}(t)$ is found and marked as $t_{3,dec}$. Then, the minimum in the motor velocity between $t_{1,dec}$ and $t_{3,dec}$ is detected and associated with $t_{2,dec}$ (second dashed line). Typically, $t_{2,dec}$ and $t_{3,dec}$ are close together.

Approximating the load-side velocity in the time interval of interest in the acceleration phase is trivial because without gravity the load should be at rest, so the velocity is zero (Marton and Lantos, 2009). For the deceleration phase it can be assumed that the load velocity is constant and identical to $\Omega_M(t_{1,dec})$ (black line). While Villwock (Villwock and Pacas, 2009) achieved good results with this approximation, it was found that in a real setting with friction in the driven mechanics a large error is introduced. In Fig. 2 this error can be quantified by comparing the surface areas between the green and black line, resp. between the

red and green line in the time interval marked by the dashed lines.

Now, the accelerometer comes into the picture. It is mounted on the translationally moving load and measures accelerations in three axes. The component in the direction of motion $a(t)$ serves to obtain the velocity between the dashed lines from numeric integration of discrete-time signals:

$$\hat{\Omega}_{\mathrm{L},k+1} = \hat{\Omega}_{\mathrm{L},k} + 2\pi i a_k T_{\mathrm{s}} / c_{\mathrm{f}}. \tag{2}$$

In this equation ˆ stands for the estimate and T_{s} for the sampling time. The time at sampling instant k, kT_{s} is shortened by the index k.

At $kT_{\mathrm{s}} = t_{1,\mathrm{dec}}$ the velocity could be initialized to the current motor measurement, but since this would depend on one single, noisy measurement a better alternative is to utilize also the common movement of motor and load during the acceleration phase. The sensor fusion of motor position measurement and accelerometer measurement could be realized via Kalman filtering (Shim et al., 1998), or since the calculation is performed offline Kalman smoothing is also possible (Särkkä, 2013). Here, the acceleration is simply integrated and the known motor velocity is used as a feedback:

$$\hat{\Omega}_{\mathrm{L},k+1} = (1-\varepsilon)\left[\hat{\Omega}_{\mathrm{L},k} + 2\pi i a_k T_{\mathrm{s}} / c_{\mathrm{f}}\right] + \varepsilon\Omega_{\mathrm{M},k}. \tag{3}$$

ε is a tuning factor that is adapted manually to adjust the dynamics of the estimate.

Since the accelerometer outputs the data with a certain, a priori unknown offset $\overline{a}$:

$$a_{\mathrm{raw},k} = a_k + \overline{a}, \tag{4}$$

this offset must be determined and compensated. We can utilize the fact that right before and after the experiment the velocity is known to be equal and zero:

$$\hat{\Omega}_{\mathrm{L}N} = \hat{\Omega}_{\mathrm{L}0} + \frac{2\pi i T_{\mathrm{s}}}{c_{\mathrm{f}}}\left[a_0 + a_1 + \cdots + a_{N-1} + N\overline{a}\right]. \tag{5}$$

With $\hat{\Omega}_{\mathrm{L}N} = \hat{\Omega}_{\mathrm{L}0} = 0$ (5) can be solved for $\overline{a}$, which is then subtracted from a_{raw}.

Another essential preparation step is the synchronisation of signals in time. Since the mobile sensor for acceleration measurement is started remotely via a non-realtime connection, the acceleration may have a time shift. For time synchronisation the cross correlation between the acceleration signals from the two sensors (motor and accelerometer) is maximized:

$$lag = \arg\max_m \sum_{k=-\infty}^{k=\infty}\left[\frac{2\pi i a_{k+m}}{c_{\mathrm{f}}} \frac{\Omega_{\mathrm{M},k+1} - \Omega_{\mathrm{M},k}}{T_{\mathrm{s}}}\right]. \tag{6}$$

This way the time lag is determined and the first *lag* samples of a_k are discarded before the above calculations are carried out.

3 EXERIMENTAL SETUP

For the experimental validation the testbed shown in Fig. 3 is used. A synchronous motor of the type MCS 12L20 with a rated power of 2.8 kW and a rated torque of 13.5 Nm is driven by an 9400 servo inverter, both from Lenze. It is connected to a belt drive of 2.20 m length by a coupling with adjustable backlash. The load allows for weight adjustment, but in these experiments a constant load of 11 kg is chosen. On the load-side of the backlash coupling a rotary multiturn encoder 'ATD 2B A 4 Y26' from Baumer Thalheim is mounted. The resolution of the encoder is 17 bits/rev. Servo inverter and encoder are connected to the main controller, '3200 C' from Lenze via EtherCAT.
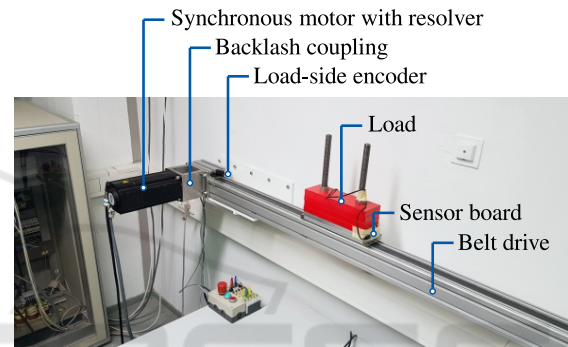

Figure 3: Experimental setup.

Figure 4 shows the backlash coupling, which works similar to the one described in (Villwock, 2007). Ball bearings have been integrated to facilitate the alignment. The gap width can be adjusted in steps: $0°, 0.5°, \cdots, 4.5°, 5°, 6°, \cdots, 20°$. This range of adjustable values is comparable to other couplings or gearboxes with adjustable deadzone (Dagalakis and Myers, 1985; Schoeling and Orlik, 2000; Merzouki et al., 2006; Rostalski et al., 2007). In (Merzouki et al., 2006) the deadzone can even be extended up to 24°. Industrial gearboxes have a motor-side backlash angle in a similar range, typically more for high transmission ratios (Lenze, 2020).

The mobile sensor is attached to the load with an ordinary tape. Figure 5 shows a detailed view of the sensor board. It is based on an Arduino ESP32 NodeMCU from Espressif with dual-core controller running at 80 MHz and 802.11 b/g/n Wi-Fi functionality. The lower PCB has been added to integrate three SRAM devices 'IS62WVS2568FBLL-20NLI' with 2 Mb, 20 MHz as a data buffer. Also, the MEMS (micro-electromechanical systems) IMU 'LSM6DS3' is mounted on the lower PCB. It is configured to measure accelerations in three axes with a resolution of 16 Bits at ± 2g full range, at a nominal noise level of $90\mu g / \sqrt{\mathrm{Hz}}$.
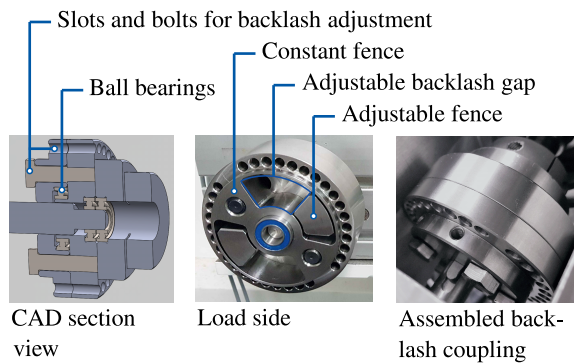
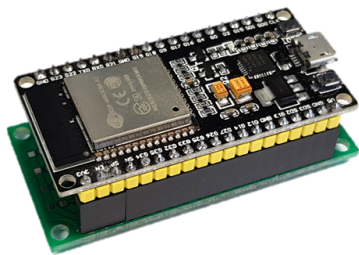Figure 4: Coupling with adjustable backlash.

Figure 5: Sensor board with MEMS IMU and Wi-Fi data transmission.

In Fig. 6 the principle of data transmission is shown. Real-time operating system FreeRTOS[TM] (Amazon Web Services, Inc., 2020) is running on the sensor board with two tasks, one for reading the measurements from the IMU and storing them in the SRAM devices and one for transmitting the data via Wi-Fi to the receiver. Reading the accelerations from the sensor can be synchronized with the clock of the actual measurement, which can be set in steps up to 1.66 kHz. In this case it is initiated by an interrupt from the sensor. Alternatively, an arbitrary sampling rate can be realized by a hardware timer interrupt. It was found that tolerances of the sensor sampling rate lead to problems in time synchronisation. For that reason the sensor is configured to measure at 1.66 kHz, while the data are recorded asynchronously at 1 kHz. This leads to time jitter, but aliasing is prevented by a low-pass filter at 400 Hz inside the IMU.

Data are transmitted to a receiver board via Wi-Fi Direct mode, which allows the simultaneous connection of several sensor boards without a wireless router. The receiver is also an ESP32, which is connected to the computer over USB.

4 EXPERIMENTAL RESULTS

In this section experimental results are reported for backlash identification. Firstly, in deceleration phase
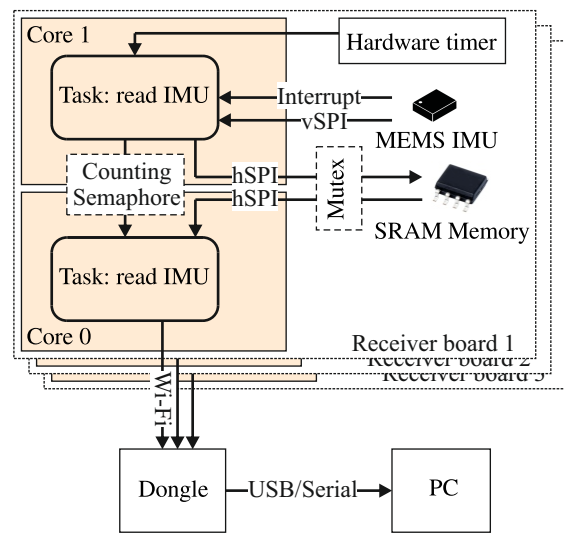

Figure 6: Schematic of the data transmission from the mobile sensor boards to the PC.

without accelerometer, secondly in acceleration phase with zero load velocity and thirdly, in deceleration phase with the mobile sensor unit.

For the identification in deceleration phase without accelerometer identified backlash angles are shown against those that have been configured in the backlash coupling in Fig. 7. Measurements have been repeated for five motor orientations spread equally over one rotation. This procedure ensures that the identification works not only for one particular orientation. In addition, as a reference the backlash values have been measured by the help of the load-side encoder (black line). For this experiment the motor-side part of the backlash coupling was fixed and the load-side position was rotated slowly by hand, while the minimum and maximum encoder readings were recorded.

The fact that the reference measurement is almost an identity line confirms that the backlash coupling has been machined accurately, although the actual width is always approximately $0.5°$ too low. The identification result is far above the correct value, for most widths even exceeding 200 %. This can be explained by the error due to neglecting the deceleration of the load as already shown in Fig. 2.

The result for the acceleration phase is shown in Fig. 8. These experiments reveal a high accuracy and repeatability which suggests a clear superiority of the method. However, it is less robust to sources of disturbing torques not considered explicitly. For example, position-dependent friction could lead to similar drops in the velocity causing confusion with the backlash-induced effect. Also, if due to a slight inclination of the linear drive there is a small gravity
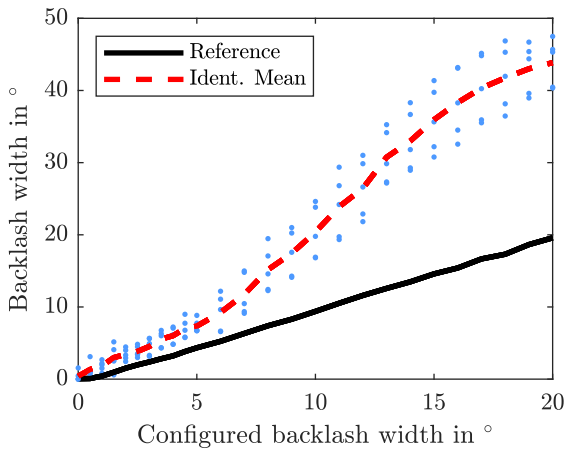
Figure 7: Identified vs. configured backlash width when the load velocity is assumed to be constant and the backlash is identified in the deceleration phase.

torque, the load acceleration will depart from zero during the measurement or the load might leave the one end of the backlash gap prior to the measurement. It is expectable that it could even become impossible to detect $t_{2,acc}$. So, although the results in the acceleration phase are good, it is expectable that this method is not robust and suffers from similar problems as the methods cited above that make certain assumptions about the load-speed.
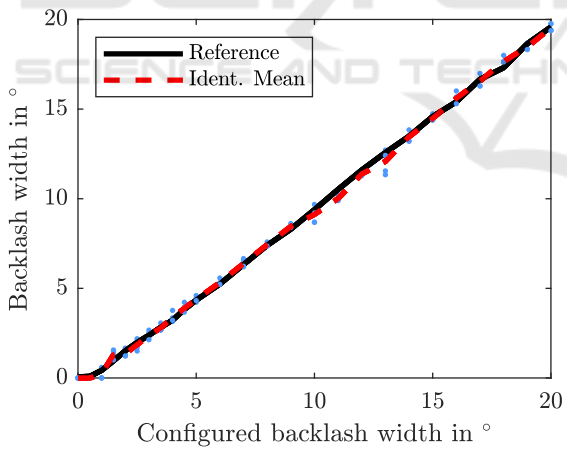

Figure 8: Identified vs. configured backlash width when the load velocity is assumed to be constant and the backlash is identified in the acceleration phase.

In the following, the results with accelerometer are reported. For an angle of $10°$ the results of the time synchronisation step are shown in Fig. 9. In this figure as well as in all other experiments a clear maximum can be seen and time synchronisation is readily possible.

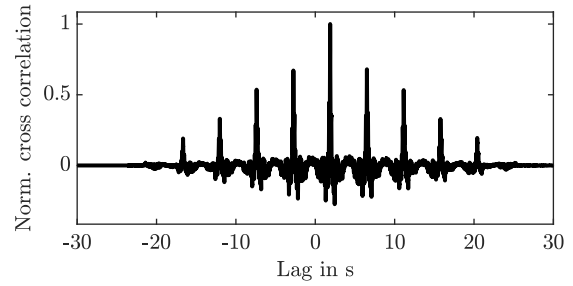After time synchronisation and drift elimination the velocity could be obtained from the accelerome-

Figure 9: Cross correlation between accelerometer measurement $a(t)$ and numerically differentiated motor velocity $\Omega_M(t)$.

ter with only a minor error as shown in Fig 10. Although only the velocities before and after the five movements are used for calibration, both graphs are in good agreement. But this free integration result is not actually needed and only shown as a verification. Instead the velocity is estimated as explained above with the result given in Fig. 11.
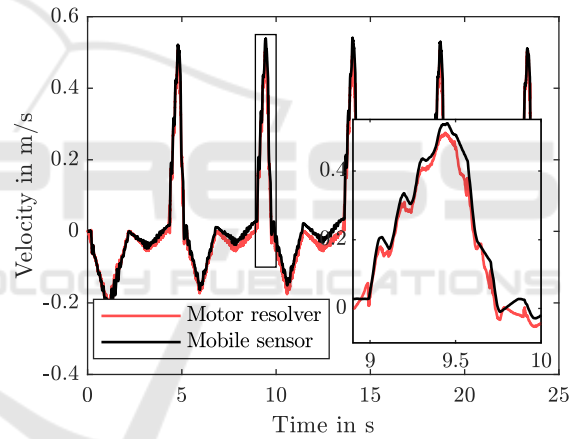

Figure 10: Velocity obtained from motor encoder $\Omega_M(t)$, resp. by integration from the mobile accelerometer.

For the same $10°$ recording as in Figs. 9 and 10 the velocities of the three different sources are shown. ε is set to 5%. Apparently, the accelerometer is in good agreement with the encoder in the deceleration phase while the backlash gap is traversed.

This impression is confirmed by the other experiments, see Fig. 12. Backlash identification is possible with low variance and high repeatability, albeit less good than in the acceleration phase, compare Fig. 8. Some of the results for $1.5°$ or less are erroneous because the time t_2 could not be extracted safely, possibly because the effect of the impact is less pronounced for small backlash widths. This can be observed in Fig. 7, too.
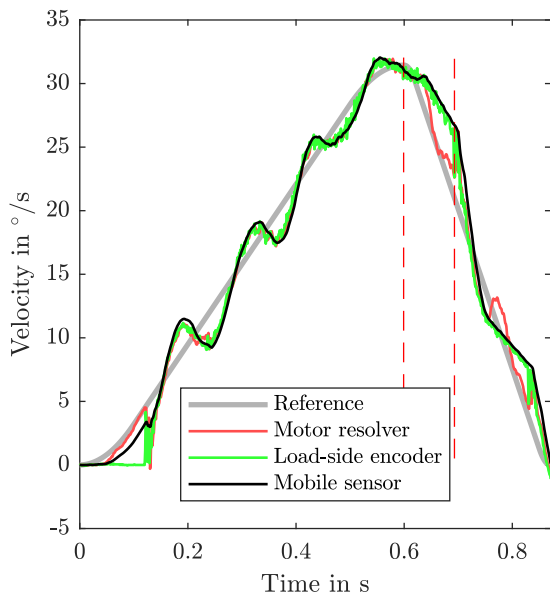
Figure 11: Velocities of an exemplary experiment with 10° backlash setting with acceleration sensor.
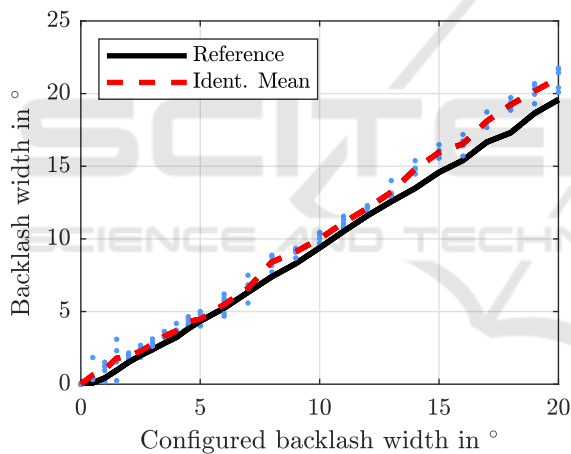

Figure 12: Identified vs. configured backlash width when the load velocity is obtained from the accelerometer, deceleration phase.

5 DISCUSSION

The presented approach towards backlash identification was shown to provide a high accuracy, especially for high backlash angles. This is remarkable as the effort and cost of installing the temporary sensor board at the load is small and it is not necessary to synchronize the different sensors in time. Apparently, the belt elasticity does not impair the measurements significantly. Many applications as listed above could benefit from such a mobile sensor for backlash identification. Although not confirmed experimentally, it can

be expected that small disturbances, such as gravity should not impair the identification significantly, because they are detected by the IMU.

Only in the low backlash domain of $1.5°$ or less the commutation times could not always be detected correctly leading to scattering of the results. Furthermore, the experiments have shown that machining inaccuracies in the backlash coupling lead to angle dependencies and tolerances in the range of $0.5°$. Therefore, the validation of the methods is also limited in accuracy and scattering of the measurements can partly be attributed to machining, not to the identification method. The results could be improved by averaging several measurements, which was not taken into account here.

It is astonishing how (Marton and Lantos, 2009) could achieve identification tolerances of only a few percent for backlash angles of $0.47°$, resp. $0.35°$. In (Han et al., 2016), too, accuracies of a few percent are achieved for $1°$. A possible explanation might be the idealized setup in their experiments contrasting with the more industry-like setup of our testbed.

It remains to be investigated if the results are equally good for a real gearbox instead of the backlash coupling. Possibly, oil between the teeth and the interplay of the multiple gear ranges could hinder a clear detection of the commutation times. Also, if the transmission ratio is high and accordingly the load velocity is slow, it could become increasingly difficult to reconstruct the load velocity from the accelerometer measurement.

Future works should investigate the applicability of MEMS gyroscopes for purely rotary settings. With a sensor board like the one used in this work it is possible to capture also rotating parts with little effort.

6 CONCLUSIONS

In this paper a method for backlash identification in electric drive trains has been proposed. It is tailored to electromechanical motion systems with rotary motor and translationally moving load. A mobile sensor board with IMU is mounted temporarily on the load and transmits the measured accelerations via Wi-Fi, thus requiring no cabling. Is was shown in experiments with an adjustable backlash coupling that high accuracies can be achieved even if the load-side friction and inertia are unknown, which has so far been a challenge with series sensor equipment. The testbed used for the experiments consists of industrial equipment, except for the coupling with adjustable backlash. It must still be investigated if similar results can be achieved with a gearbox instead of the back-

lash coupling. The IMU measurement can be initiated manually independent of the hardware that controls the motor, because time synchronisation is possible based on the recorded signals.

ACKNOWLEDGEMENTS

REFERENCES

Amazon Web Services, Inc. (2020). FreeRTOS^{TM} - real-time operating system for microcontrollers. https://www.freertos.org/index.html, accesssed: Feb. 2020.

Calvini, M., Carpita, M., Formentini, A., and Marchesoni, M. (2015). Pso-based self-commissioning of electrical motor drives. *IEEE Transactions on Industrial Electronics*, 62(2):768–776.

Dagalakis, N. G. and Myers, D. R. (1985). Adjustment of robot joint gear backlash using the robot joint test excitation technique. *The international journal of robotics research*, 4(2):65–79.

Friedland, B. (1997). Feedback control of systems with parasitic effects. In *Proceedings of the 1997 American Control Conference (Cat. No. 97CH36041)*, volume 2, pages 937–941. IEEE.

Gebler, D. and Holtz, J. (1998). Identification and compensation of gear backlash without output position sensor in high-precision servo systems. In *IECON'98. Proceedings of the 24th Annual Conference of the IEEE Industrial Electronics Society (Cat. No. 98CH36200)*, volume 2, pages 662–666. IEEE.

Han, Y., Liu, C., and Wu, J. (2016). Backlash identification for PMSM servo system based on relay feedback. *Nonlinear Dynamics*, 84(4):2363–2375.

Itoh, M. (2008). Torsional vibration suppression of a twin-drive geared system using model-based control. In *2008 10th IEEE International Workshop on Advanced Motion Control*, pages 176–181. IEEE.

Lagerberg, A. (2001). A literature survey on control of automotive powertrains with backlash. Technical Report R013/2001, Control and Automation Laboratory, Chalmers University of Technology, Göteborg, Sweden.

Lagerberg, A. and Egardt, B. (2005). Model predictive control of automotive powertrains with backlash. *IFAC Proceedings Volumes*, 38(1):1–6.

Lenze (2020). Product-related documentation. https://www.lenze.com/en-de/services/knowledge-base/product-related-documentation/, accesssed: Feb. 2020.

Marton, L. and Lantos, B. (2009). Friction and backlash measurement and identification method for robotic arms. In *2009 International Conference on Advanced Robotics*, pages 1–6. IEEE.

Merzouki, R., Davila, J. A., Cadiou, J. C., and Fridman, L. (2006). Backlash phenomenon observation and identification. In *2006 American Control Conference*, pages 3322–3327. IEEE.

Nordin, M. and Gutman, P.-O. (2000). Nonlinear speed control of elastic systems with backlash. In *Proceedings of the 39th IEEE Conference on Decision and Control (Cat. No. 00CH37187)*, volume 4, pages 4060–4065. IEEE.

Nordin, M. and Gutman, P.-O. (2002). Controlling mechanical systems with backlash – a survey. *Automatica*, 38(10):1633–1649.

Popp, E., Tantau, M., Wielitzka, M., Ortmaier, T., and Giebert, D. (2019). Frequency domain identification and identifiability analysis of a nonlinear vehicle drivetrain model. In *2019 18th European Control Conference (ECC)*, pages 237–242. IEEE.

Ravanbod-Shirazi, L. and Besançon-Voda, A. (2002). Backlash identification: a two step approach. *IFAC Proceedings Volumes*, 35(1):85–90.

Reddy, P., Darokar, K., Robinette, D., Shahbakhti, M., Blough, J., Ravichandran, M., Farmer, M., and Doering, J. (2019). Control-oriented modeling of a vehicle drivetrain for shuffle and clunk mitigation. Technical report, SAE Technical Paper.

Rostalski, P., Besselmann, T., Barić, M., Belzen, F. V., and Morari, M. (2007). A hybrid approach to modelling, control and state estimation of mechanical systems with backlash. *International Journal of Control*, 80(11):1729–1740.

Särkkä, S. (2013). *Bayesian filtering and smoothing*, volume 3. Cambridge University Press.

Schoeling, I. and Orlik, B. (2000). Control of a nonlinear two-mass system with uncertain parameters and unknown states. In *IEEE Industry Applications Conference (Cat. No. 00CH37129)*, volume 2, pages 1096–1103. IEEE.

Shim, H., Kochem, M., and Tomizuka, M. (1998). Use of accelerometer for precision motion control of linear motor driven positioning system. In *IECON'98. Proceedings of the 24th Annual Conference of the IEEE Industrial Electronics Society (Cat. No. 98CH36200)*, volume 4, pages 2409–2414. IEEE.

Specht, R. (1986). Ermittlung von Getriebelose und Getriebereibung bei Robotergelenken mit Gleichstromantrieben. *VDI-Berichte*, (598):71–83.

Tao, G. and Kokotovic, P. V. (1996). *Adaptive control of systems with actuator and sensor nonlinearities*. John Wiley & Sons, Inc.

Villwock, S. (2007). *Identifikationsmethoden für die automatisierte Inbetriebnahme und Zustandsüberwachung elektrischer Antriebe*. PhD thesis, Universität Siegen.

Villwock, S. and Pacas, M. (2009). Time-domain identification method for detecting mechanical backlash

in electrical drives. *IEEE Transactions on Industrial Electronics*, 56(2):568–573.

Zemke, S. (2012). *Analyse und modellbasierte Regelung von Ruckelschwingungen im Antriebsstrang von Kraftfahrzeugen*. PhD thesis, Leibniz Universität Hannover.

Zhang, J., Zhang, H., and Xiao, X. (2018). New identification method for backlash of gear transmission systems. In *2nd IEEE Advanced Information Management, Communicates, Electronic and Automation Control Conference (IMCEC)*, pages 378–382. IEEE.